

# An Environmentally Benign, Highly Efficient Catalytic Reduction of *p*-Nitrophenol using a Nano-Sized Nickel Catalyst Supported on Silica-Alumina

Islam Hamdy Abd El Maksod,<sup>a,d</sup> Eman. Z. Hegazy,<sup>a,d</sup> Sayed. H. Kenawy,<sup>b</sup> and Tamer S. Saleh<sup>c,\*</sup>

<sup>a</sup> Physical Chemistry Department, National Research Centre Dokki, El Behouth Street, Dokki, Cairo 12622, Egypt

<sup>b</sup> Ceramic Department, National Research Centre Dokki, El Behouth Street, Dokki, Cairo 12622, Egypt

<sup>c</sup> Green Chemistry Department, National Research Centre, Dokki, El Behouth Street, Dokki, Cairo 12622, Egypt  
Fax: (+20)-2-3337-0931; e-mail: tamsaid@yahoo.com

<sup>d</sup> Chemistry Department, Faculty of Science, King Abdul Aziz Univesity, Jeddah 21533, Saudi Arabia

Received: December 17, 2009; Revised: March 29, 2010; Published online: April 26, 2010

**Abstract:** A green and effective method is reported for the reduction of *p*-nitrophenol to *p*-aminophenol using a nano-sized nickel catalyst supported on silica-alumina in the presence of hydrazine hydrate as an alternative source of hydrogen. It was found that nickel loaded on a silica-alumina support is a very effective catalyst in the hydrogenation of *p*-nitrophenol to *p*-aminophenol. Thus it attained 100% conversion in only 69 seconds instead of 260 seconds for commercial Raney nickel. In addition, the possibility to reuse it more than one time with great efficiency gives it another advantage over commercial Rainey nickel which cannot be used more than once. This economical and environmentally friendly

method provides a potentially new approach for the synthesis of the intermediate product of paracetamol in industry, which overcomes the drawbacks of the known reduction methods. The prepared catalysts were fully characterized by X-ray diffraction (XRD), scanning electron microscopy (SEM), energy dispersive X-ray (EDX), and electron spin resonance (ESR) techniques.

**Keywords:** *p*-aminophenol; catalytic activity; electron spin resonance (ESR); nano-sized nickel catalyst; scanning electron microscopy (SEM); X-ray diffraction (XRD)

## Introduction

Nickel metal catalyst loaded onto SiO<sub>2</sub> or Al<sub>2</sub>O<sub>3</sub> has been used as the catalyst in hydrogenation reactions only as the separate oxides.<sup>[1–8]</sup> These reactions are considered to be highly important, especially for many vital industries. For example, the hydrogenation of edible oil is one of the most important hydrogenation reactions in the food industry.<sup>[7,8]</sup>

*p*-Aminophenol is considered to be a very important intermediate in the manufacture of many analgesic and antipyretic drugs, such as paracetamol, acetanilide, phentacin, etc.<sup>[9–15]</sup> It is also used as a developer in photography (under trade names of activol or azol), in addition to its uses in the chemical dye industries.<sup>[10–16]</sup> There are several methods used in the preparation of *p*-aminophenol from *p*-nitrophenol, such as (i) metal/acid reduction,<sup>[17]</sup> (ii) catalytic hydrogenation,<sup>[18]</sup> (iii) electrolytic reduction,<sup>[19]</sup> (iv) homogeneous catalytic transfer hydrogenation,<sup>[20]</sup> (v) heterogeneous catalytic transfer hydrogenation, etc.

Among all previously mentioned methods, the direct catalytic hydrogenation of *p*-nitrophenol to *p*-aminophenol was proved to be the most effective one.<sup>[15]</sup> Raney nickel,<sup>[21]</sup> nano-sized nickel<sup>[22]</sup> and several noble metal catalysts, such as Pd/C,<sup>[15]</sup> have been used as catalysts for this reaction. Due to their lower cost and higher catalytic activity, supported nickel catalysts are widely used in such reactions.<sup>[15–21]</sup>

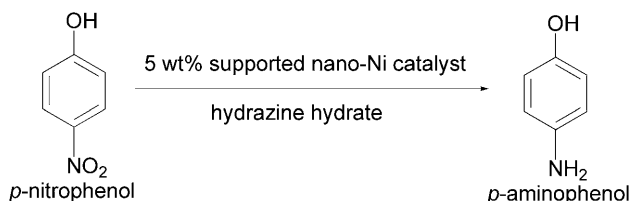
Although nickel catalysts are used in the hydrogenation reactions, only few recent studies have been carried out on the hydrogenation of *p*-nitrophenol over nano-sized, supported nickel metal catalysts.<sup>[30–33]</sup> To the best of our knowledge the catalytic behavior of metallic nickel loaded on a mixed SiO<sub>2</sub>-Al<sub>2</sub>O<sub>3</sub> solid has not yet been investigated before.

The present investigation reports the utility of hydrazine hydrate as an alternative source of hydrogen with the supported nano-sized nickel catalysts as a system for the reduction of aromatic nitro compounds taking *p*-nitrophenol as an example. H<sub>2</sub> and N<sub>2</sub> are the only products of the catalytic decomposition of

hydrazine hydrate over the nano-sized nickel catalyst in this reduction system.

## Results and Discussion

The hydrogenation of *p*-nitrophenol into *p*-aminophenol was performed using 5 wt% Ni catalyst, supported on the precalcined supports; SA-500, SA-1000 and SA-1500. The reaction proceeds according to Eq. (1).



The hydrazine in the previous reaction acts as a hydrogen donor. In addition, the supported nickel catalyst acts as a bifunctional catalyst. Thus, it firstly, decomposes hydrazine into  $H_2$  and  $N_2$ . In addition, the nickel acts as a catalyst for the hydrogenation of *p*-nitrophenol (PNP) using the nascent hydrogen produced from the previous step.

During the hydrogenation process, a change in color was observed. Thus, a change from the yellow color of PNP into a green color (intermediate A) was first observed. After that, the discharge of all colors (PAP) occurred, accompanied with 100% conversion. The mechanism of this reaction was proposed and confirmed in our previous work.<sup>[33]</sup>

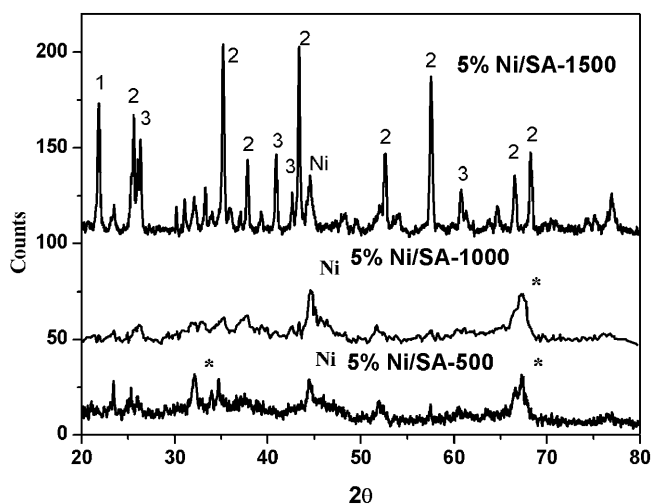


**Figure 1.** XRD diffractograms of 5 wt% Ni loaded on SA-500, SA-1000 and SA-1500, where 1 is crystallite, 2 is corundum, 3 is mullite, and \* is  $\gamma$ - $Al_2O_3$ .

The proposed mechanism enables us to follow the reaction by the changes in color. This makes the expression of the catalytic activity as the time to reach 100% conversion the best choice for this reaction.

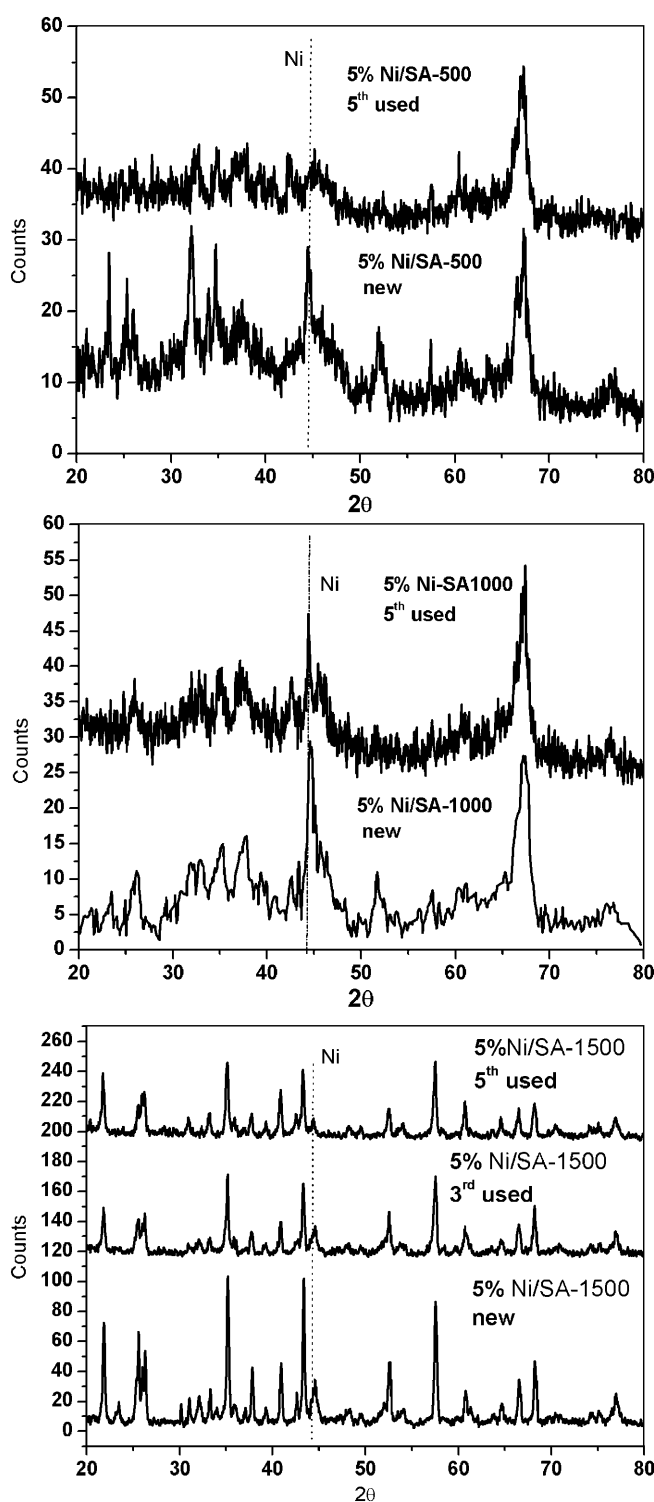


**Figure 2.** XRD diffractograms of 5 wt% Ni loaded on SA-500, SA-1000 and SA-1500 supports before and after several successive uses in the hydrogenation of *p*-nitrophenol.

The supported catalysts were characterized by XRD, SEM, EDX, ESR and measurements of the catalytic activity.

### XRD Investigation of Different Solids

A poorly crystallized alumina, together with the main diffraction line of metallic nickel are the main features of the diffractograms of 5 wt% Ni loaded on SA-500 and SA-1000 (Figure 1). However, the diffractogram of 5 wt% Ni loaded on the SA-1500 sample consists of well crystallized  $\alpha$ -Al<sub>2</sub>O<sub>3</sub> (corundum), SiO<sub>2</sub> (cristobalite), and SiO<sub>2</sub>-Al<sub>2</sub>O<sub>3</sub> (mullite) in addition to metallic nickel.

After successive use of different samples of the catalysts, the diffractograms of the all samples (Figure 2) showed that the relative intensity of the metallic nickel phase decreases progressively as the number of

uses increases. This finding may indicate that the crystalline metallic nickel phase loses its degree of crystallinity *via* partial transformation into an amorphous phase during the hydrogenation reaction. However, in the case of the SA-1500 sample, a decrease in the degree of crystallinity of both crystalline nickel and other crystalline phases (cristobalite, corundum, and mullite) was observed after several successive uses of catalyst.

### SEM and EDX Results

Only some crystallites of alumina phases could be observed in the SEM images of 5 wt% Ni loaded on SA-500 (Figure 3) as was evidenced also by EDX analysis (Table 1) and XRD (Figure 1).

Moreover, after 5 uses, aggregation of the catalyst was observed, which is much clearer at lower magnifi-

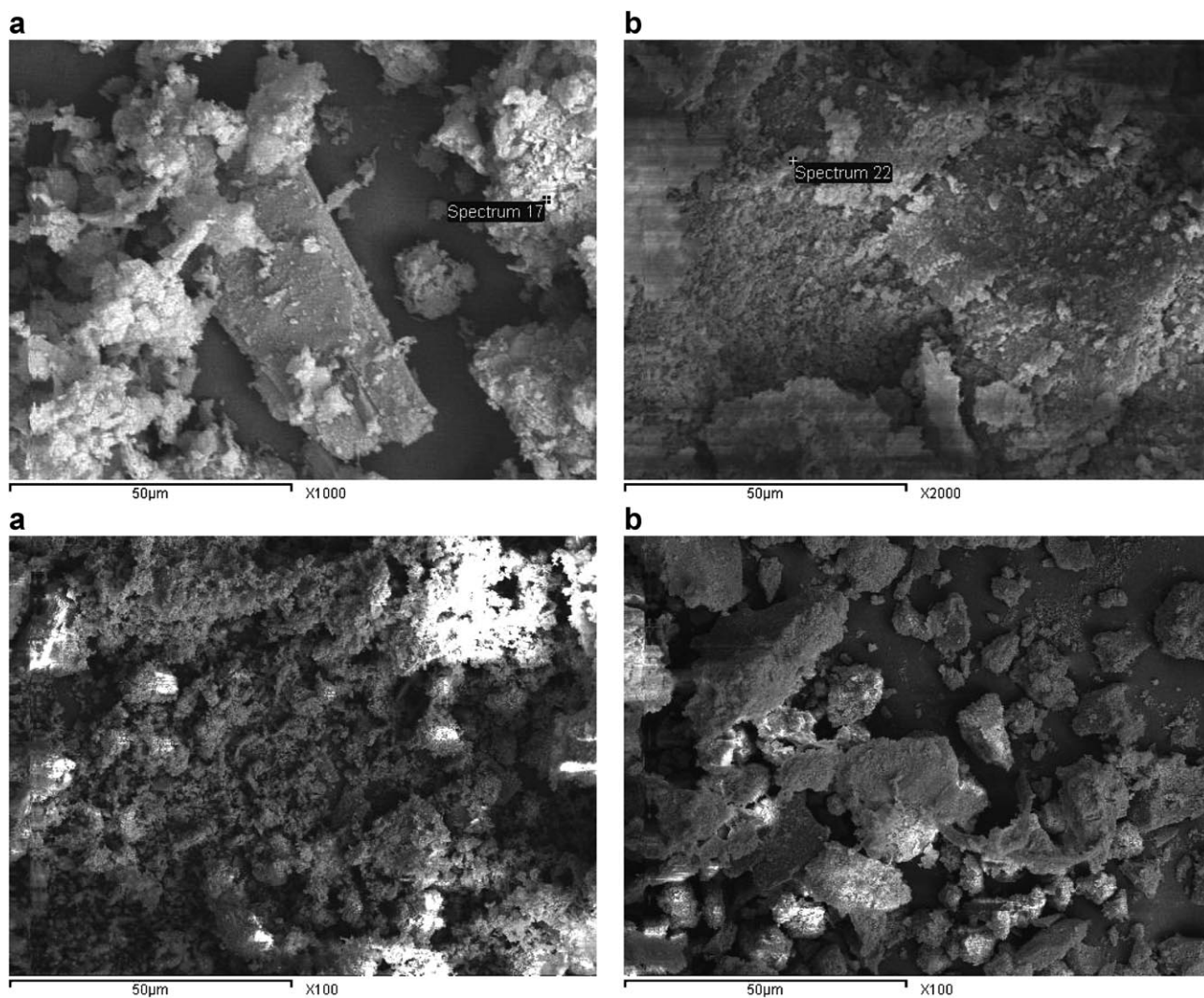


**Figure 3.** SEM images of 5 wt% Ni supported on SA-500 (a) freshly prepared and (b) after 5 successive uses in the hydrogenation reaction.

**Table 1.** EDX samples of some catalysts samples under investigation.<sup>[a]</sup>

Sample 5 wt% Ni	Si (atom%)	Al (atom%)	O (atom%)	Ni (atom%)
Bulk (calculated)	9	28	61	2
1500 °C fresh	5	39	52	5
1500 °C 5th use	31	19	50	–
1000 °C fresh	4	34	58	4
1000 °C 5th use	9	33	57	1
500 °C fresh	9	33	48	10
	–	51	41	9
500 °C 5th use	23	43	31	4
	–	61	34	6

<sup>[a]</sup> Experimentally found surface concentrations.

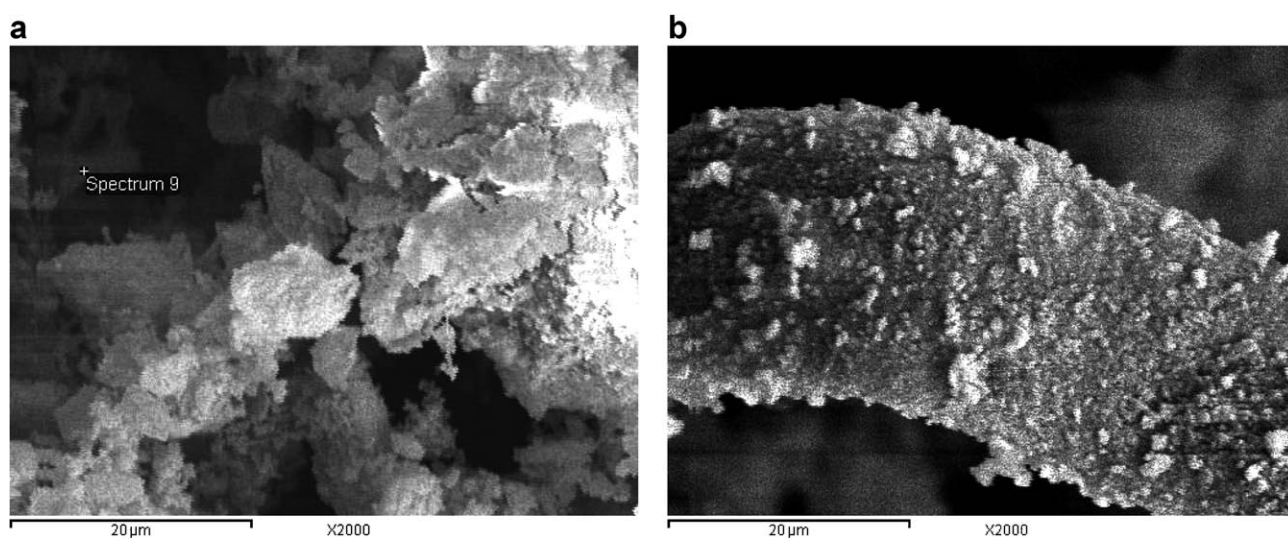
cation. The EDX analysis (Table 1) for this sample was taken from two different positions. The first position showed only the presence Al and O atoms, indicating the presence of a separate Al<sub>2</sub>O<sub>3</sub> phase, while the second position showed the presence of Si, Al and O, which is indicative for the presence of precursors of aluminosilicates.

In addition, the Si and Al surface concentrations, in the second position of the fresh catalyst, are much closer to the calculated bulk values [ $Si_{exp}$ , 9 atom%;  $Si_{cal}$ , 9 atom%,  $Al_{exp}$ , 33 atom%;  $Al_{cal}$ , 28 atom%]. On the other hand, the Ni surface concentration is much larger by 82% than the calculated bulk value [ $Ni_{exp}$ , 10 atom%,  $Ni_{cal}$ , 2 atom%]. This finding indicates that the impregnation method increases the surface atom% of Ni. This is expected for solid samples prepared by a wet impregnation method.

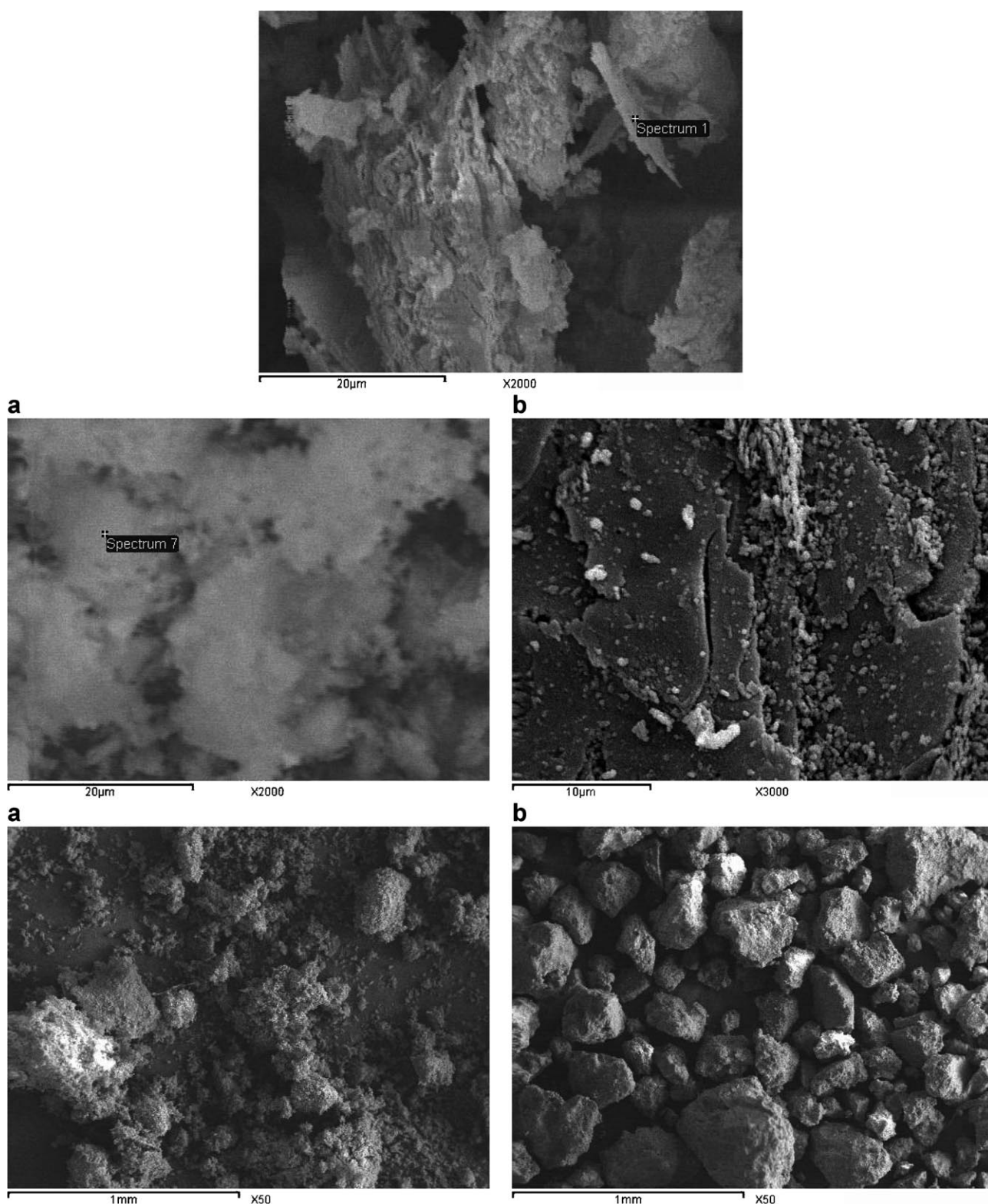
Further investigation of the SEM images of 5 wt% Ni fresh catalyst loaded on SA-1000 and after 5 uses in the hydrogenation of PNP showed that some crystallites are beginning to be formed (Figure 4). Moreover, aggregation of the catalyst after 5 successive uses was also observed, and this is accompanied by the disappearance of the crystalline shapes. The EDX analysis of this sample (Table 1) showed that there is an effective migration of Ni from the surface to the bulk on successive use (4→1 atom%). This process is accompanied also by a migration of some Si from the bulk to the surface, while, Al and O remained almost unchanged. It can be also observed that the surface atom concentrations of Si, Al, O and Ni atoms are much closer to the calculated bulk values after 5 successive uses, which may affect the specific catalytic activity of this catalyst, as will be seen later in the section on catalytic activity.

Figure 5 shows the images of 5 wt% Ni catalyst loaded on SA-1500 before and after 5 uses, compared with the bare support sample. The clear formation of highly crystalline forms of the support was observed. The particles of the catalyst underwent an observable aggregation after several uses. The EDX analysis showed that the Ni migrates completely from the surface to the bulk (5→~0.0 atom%), while a high migration of Si from the bulk to the surface is observed (5→31 atom%). The Al atoms migrates also, but this time from the surface to the bulk (39→19 atom%). These findings may be explained by assuming the collapse of the crystalline forms of the support which was confirmed previously by XRD.

From the previous observations, the following remarks may be drawn. (i) For the fresh catalyst sample, the surface concentrations of nickel loaded on SA-1500 and SA-1000 reach 5 and 4 atom%, re-



**Figure 4.** SEM images of 5 wt% Ni loaded on SA-1000, (a) freshly prepared and (b) after 5 successive uses in the hydrogenation reaction.



**Figure 5.** SEM images of the bare support SA-1500 (*top*), and (a) freshly prepared 5% wt% Ni-SA-1500 and (b) the same after 5 successive uses in the hydrogenation reaction.

spectively. These values are closer to the calculated values of loaded Ni (2 atom%), comparing with the high value of surface Ni concentration (10 atom%)

loaded on SA-500. This means that the Ni atoms are not equally distributed between surface and bulk, and are much more highly concentrated on the surface.

This may be explained by assuming that the interaction between Ni atoms and the amorphous support is higher than that with crystalline support. In other words, as the degree of crystallinity of the support increases the interaction between Ni and the support decreases which was formerly observed from XRD and SEM results. (ii) It can be generally observed that, as the calcination of the support increases, the distribution of surface Si and Al deviates from the calculated bulk values. As a consequence of successive uses of the catalyst, a migration of both Si and Al and even O occurs. The migrating atom concentrations were found to be much closer to the calculated bulk values, i.e., as the catalyst is being used, the support transforms into the amorphous phase. (iii) After successive use of the catalyst several times, the concentration of the surface nickel atoms decreases. This decrease is inversely proportional to the calcination temperature, reaching a minimum at 1500°C (nearly no nickel observed at EDX analysis). It was suggested that, as the degree of crystallinity of the support increases, the collapse of the crystals during the successive use of the catalyst increases. This leads to a migration of the nickel species inside the bulk. Thus, the Ni mobility is directly proportional to the degree of crystallinity of the support as can be deduced from Figure 6.

### ESR Investigation of Different Catalyst Samples

The ESR technique is usually used to characterize the paramagnetic centers in a sample where a free electron exists. In addition, it attracts more interest when these particles are diminished to the nano scale such as in our case, where nano-sized metal particles exist.

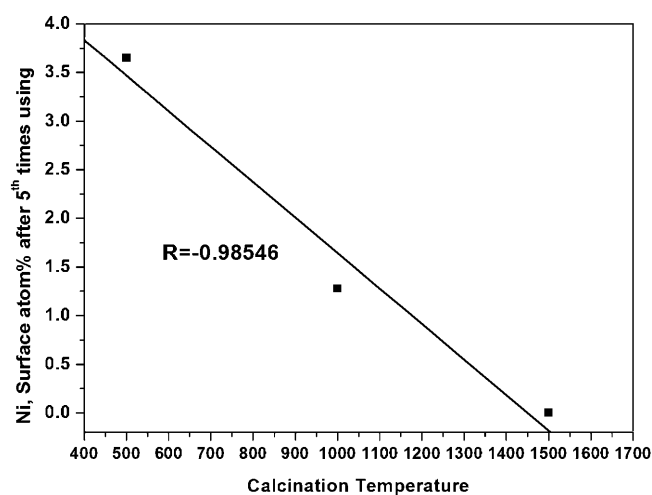


**Figure 6.** Surface Ni atom% of catalyst after 5 uses plotted using against calcination temperature.

Moreover, Kawabata in 1970<sup>[35]</sup> demonstrated his seminal relation hypothesizing that the broadening of the ESR signal of nano-metal particles is suffering from a quantum size effect and can be correlated to the size of the nano-metal particle. Accordingly, a direct relationship between the line width  $\Delta H_{pp}$  (or peak to peak width) of the signal of the nanoparticle in the ESR spectrum and its particle size is given by the relation  $d = a \cdot (\Delta H_{pp})^{0.5}$ , where  $d$  is the particle size in nm,  $\Delta H_{pp}$  is the line width of the ESR signal in mT, and  $a$  is the proportionality constant.

The proportionality constant  $a$  for, in our case, nickel metal was found to be 1.2.<sup>[8]</sup> This relation enables us to estimate correctly the average particle size of nickel even when it is not existing in a crystalline form. Thus, Figure 7 demonstrates the ESR spectra of samples under investigation under different calcination temperatures and after successive uses. From these spectra one can observe that the characteristic signal of nickel metal appears at  $g = 2.2$  and exists in all samples.<sup>[8]</sup> Moreover, additional overlapping, low magnetic field signals appeared in different samples. These lower magnetic field signals were assumed to be attributed to the existence of strain between the nano-nickel particles.<sup>[33,35-36]</sup>

We assume that the disappearance of this strain means that nano-sized nickel particles are well separated among each other. In other words, the interaction between the metal and the support is minimal. According to this assumption, one can observe easily from the ESR spectra of the samples (Figure 7) that the freshly prepared nickel catalyst supported on SA-1500 exhibits no strain and this means that the interaction between metal and the support is minimal. XRD diffractograms of the catalyst (Figure 2) show also that it has a larger degree of crystallinity.

The particle size decreases progressively on increasing the number of uses (Figure 7). A decrease of 30% after using the catalyst supported on SA-1500 was observed. Furthermore, the Ni phase turned into an almost amorphous phase which agreed well with the XRD investigations.

Moreover, using the calculation of particle size by Kawabata's equation (labeled on each sample on Figure 7), it can be observed that, as the number of successive uses of catalyst in the hydrogenation reaction increases, the particle size of nickel decreases. In other words, the amorphous nature of nickel is increasing which was previously concluded from XRD diffractograms.

In contrast to the previous observations, the particle size of Ni in the catalyst sample whose support was SA-500 seems to be increasing after successive uses. This indicates that the mode of deactivation of this catalyst sample may suffer also from some kind of sintering.

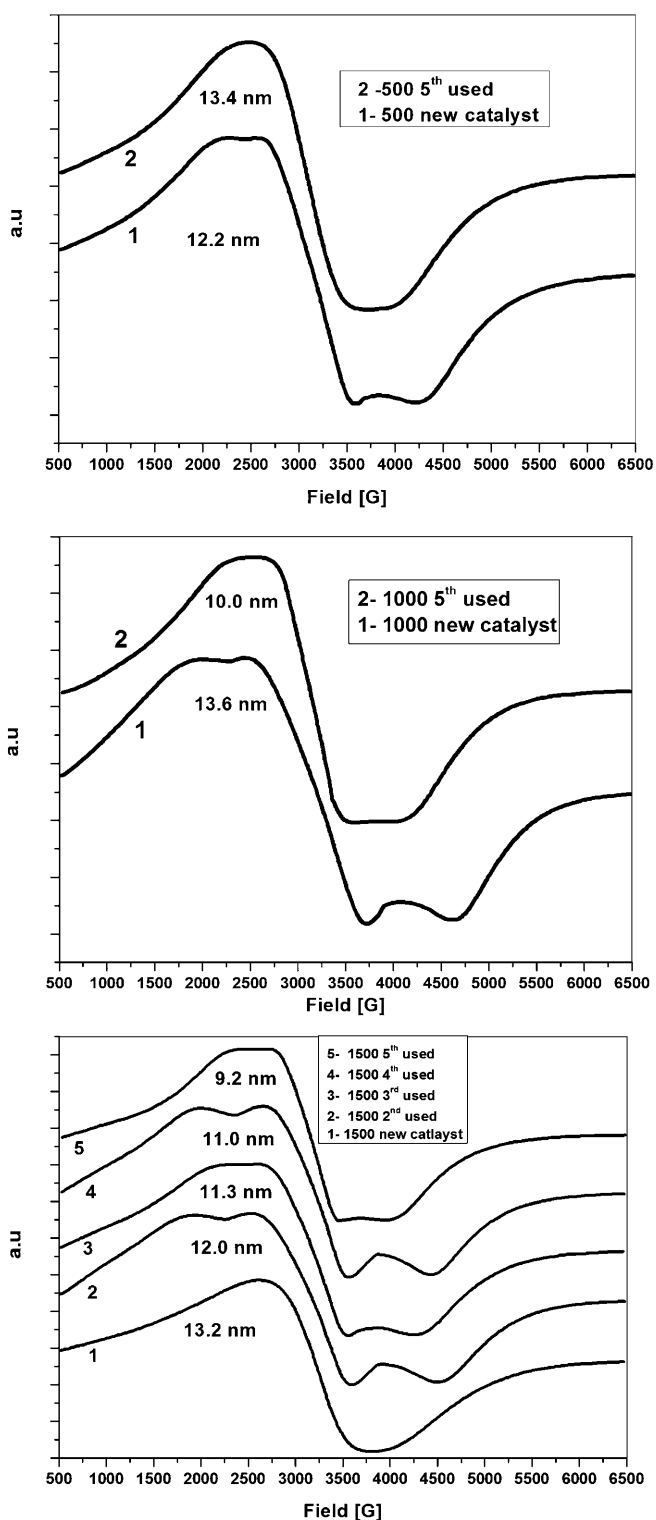


**Figure 7.** ESR spectra of different samples of 5% Ni loaded on SA-500, SA-1000 and SA-1500°C as freshly prepared catalysts and after successive cycles of use. The dimensions given in the figures are derived from Kawabata's equation.

In order to eliminate the possibility of leaching of Ni metal from the support during the hydrogenation reaction, elemental analysis for nickel in the superna-

tant was done after each experiment. The results showed that the amount of Ni leached in all samples was very small and can be neglected.

### Catalytic Activity

The catalytic activity of catalyst samples under investigation was carried out by hydrogenation of PNP into PAP. This reaction was carried out using hydrazine hydrate as hydrogen donor at 80°C.

The catalytic activity of the bare supports calcined at 500, 1000 and 1500°C (SA-500, SA-1000, and SA-1500) were examined and showed no catalytic activity. In addition the reaction with PAP with only hydrazine hydrate was also examined and showed also no reaction. Further 5 wt% Ni was loaded on the precalcined supports and reduced using hydrazine hydrate at 80–100°C.

The loaded Ni-support catalysts were then examined in the above-mentioned hydrogenation reaction. Figure 8 shows the time in seconds for 100% conversion as a function of calcination temperature of the support material.

The increase in the precalcination temperature of the support material within the 500–1500°C range led to a progressive increase in the catalytic activity (Figure 8). This was evidenced from the progressive significant decrease in the time for attaining 100% conversion. This increase in the precalcination temperature from 500 to 1500°C decreases the time for 100% conversion from 107 to about 70 seconds. The increase in crystallinity of the support material showed a parallel progressive increase in catalytic activity.

In order to make a comparison between the catalytic activity of the system investigated with the com-

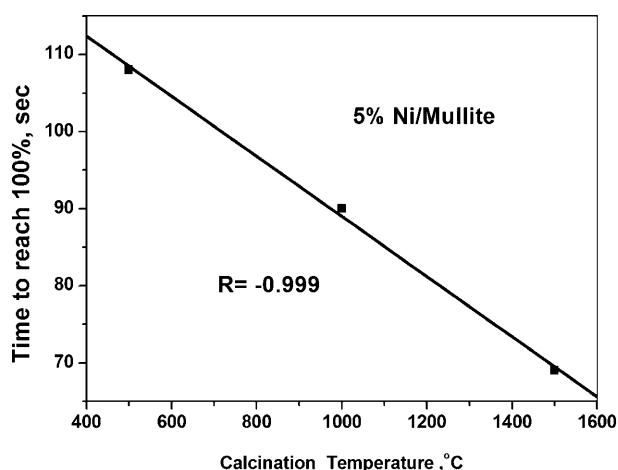


**Figure 8.** Catalytic activity of different catalysts expressed as time to reach 100% conversion against calcination temperature of the support.

mercial catalyst (Raney nickel), the hydrogenation reaction was carried out for this commercial sample under the same conditions and ratios used in other samples. The time needed to obtain 100% conversion amounted to 260 seconds instead of 69 seconds for the catalyst investigated whose support was SA-1500. In other words, the prepared catalyst showed a catalytic activity about 4-fold higher than that of Raney nickel catalyst.

In order to shed some light on the durability of the prepared catalyst, the reaction was done several successive times (5 times) and the effect of this parameter is readily observed in Figure 9. A slight decrease in the catalytic activity of the catalyst during the first 3 successive uses was observed. However, the catalyst supported on SA-500 loses most of its catalytic activity from the 4<sup>th</sup> use, while the catalysts whose supports are SA-1000 and SA-1500 lost some of their activity after 5<sup>th</sup> use. The decrease was, however, more pronounced in the case of the catalyst sample whose support is SA-1500.

This finding suggested that the catalyst whose support was calcined at 1000 °C is recommended for such reactions for its obvious durability.

Returning to EDX results which showed that the surface nickel in the sample whose support is SA-500 decreases from fresh to 5<sup>th</sup> used catalyst as (10 → 4 atom%) (Table 1). Thus it can be concluded that not all surface Ni atoms are catalytically active. In case of catalysts based on SA-1000 and SA-1500 supports, the durability is higher than that of that based on the SA-500 support. Thus, although the sharp decrease was observed in the surface Ni atoms during the reaction in case of both catalysts based on SA-1000 and SA-1500 supports (Table 1), the catalytic activity is not affected markedly. This leads us to con-

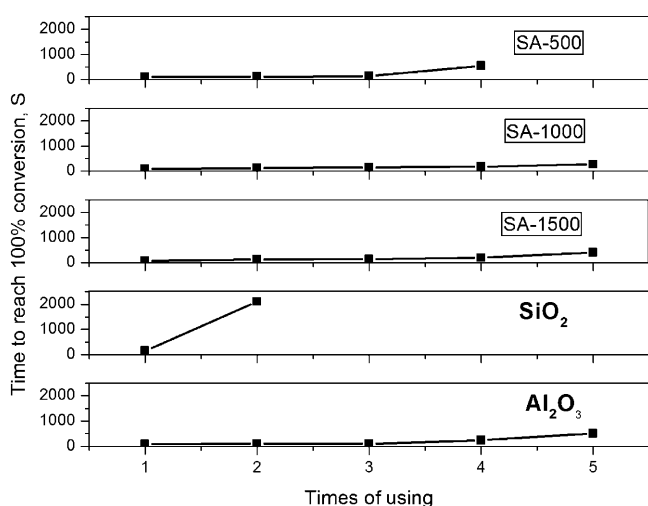


**Figure 9.** The effect of successive uses of the nickel catalyst loaded on pure SiO<sub>2</sub>, pure Al<sub>2</sub>O<sub>3</sub>, SA-500, SA-1000 and AS-1500.

clude that, in these samples, both surface and bulk nickel participates in the reaction while in the SA-500 sample only a part of surface nickel is activated. In other words, as the degree of the crystallinity of the support increases the number of active nickel species increases and hence the catalytic activity and durability increase. This may be because of the fact that, in the case of crystalline samples, diffusion of the reactants into the bulk is much easier than that with amorphous ones.

It seems that the change in the surface concentration of Ni atoms as a function of calcination temperature of the support material may have a decisive role in changing the catalytic activity. This has been probed by following the change in the catalytic activity, expressed as time to reach 100% conversion, as a function of the difference between the surface Ni of the catalyst after the 5<sup>th</sup> use subtracted from the calculated bulk concentration of Ni. The results obtained are given in Figure 10.

From Figure 10 it can be seen that the sample whose support was SA-1000, has the lowest difference to the calculated bulk values after 5 cycles of use. This may explain the higher durability of this sample. This led us to assume that as the atomic percent of Ni approaches the calculated bulk values, the catalytic activity reaches maximum.

However, we can make a comparison between the catalytic activity of 5% Ni catalyst loaded on pure SiO<sub>2</sub> and Al<sub>2</sub>O<sub>3</sub> supports with those samples under investigation. Thus, from Figure 11, it can be seen that the catalyst loaded on SA-1500 support attains the higher catalytic activity among all samples. In addition to that, it was observed also that the durability of the catalyst loaded on SA-1000 sample was the best

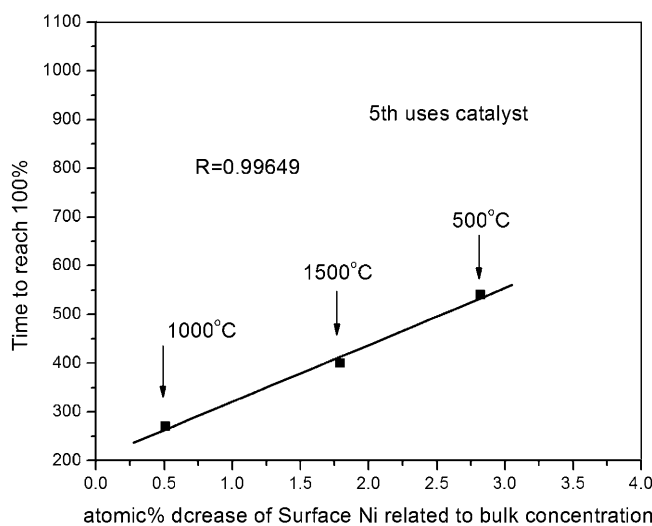


**Figure 10.** The %atom Ni after 5 uses of the nickel catalyst subtracted from the calculated bulk atom% of Ni loaded on SA-500, SA-1000 and AS-1500.

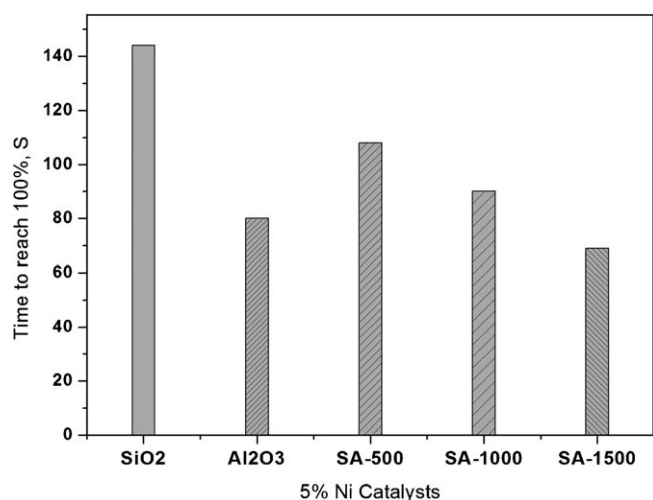


**Figure 11.** A comparison between catalytic activity of 5 wt% Ni loaded on SiO<sub>2</sub>, Al<sub>2</sub>O<sub>3</sub>, SA-500, SA-1000 and AS-1500.

compared to both pure SiO<sub>2</sub> and Al<sub>2</sub>O<sub>3</sub> and the other investigated samples<sup>[33]</sup> (Figure 9).

## Conclusions

The following conclusions can be drawn from this research:

First, nickel loaded on SiO<sub>2</sub>-Al<sub>2</sub>O<sub>3</sub> support is a very effective catalyst in the hydrogenation of *p*-nitrophenol to *p*-aminophenol. It achieved 100% conversion in only 69 seconds instead of 260 seconds for commercial Raney nickel. In addition, the possibility to reuse it more than one time with great efficiency gives it another advantage over commercial Raney nickel which cannot be used more than once.

Second, the crystallinity of the support plays a very important role in the catalytic activity of the nickel catalyst. The increase in the precalcination temperature of the support material within the range 500–1500 °C increases the degree of crystallinity of the support and also increases the catalytic activity of the catalyst.

Third, the catalyst investigated showed high durability. The optimum durability was achieved with the catalyst sample whose support was precalcined at 1000 °C (SA-1000).

Fourth, the durability is depending on the change in the physical state of the support in which the higher crystalline support is supposed to be collapsed first because the activity of it in the first run is higher. That is, the diffusion of reactants and products in and out the support will be high which results in a higher rate of collapse as evidenced by SEM images and XRD. However, the SA-1000 sample showed moderate crystallinity and less activity for the first run and

hence it shows higher durability because the physical state of the support is less affected by a lower diffusion rate.

Fifth, the mechanism of the hydrogenation reaction is proposed according to the change in color during the reaction. The change in color during the reaction makes a self indication of 100% conversion which saves the time and effort for following up the reaction.

Sixth, in comparison with 5 wt% nickel catalyst supported on single oxides<sup>[33]</sup> of SiO<sub>2</sub> and Al<sub>2</sub>O<sub>3</sub>, the nickel catalysts supported on mixed oxides were proven to be higher in both catalytic activity and durability than the catalysts supported on single oxides.

## Experimental Section

### Materials

Tetraethoxysilane (TEOS; Fluka, >98% purity), aluminum nitrate nonahydrate [Al(NO<sub>3</sub>)<sub>3</sub>·9H<sub>2</sub>O], NiSO<sub>4</sub>·7H<sub>2</sub>O (Merck), Commercial Raney nickel (Merck), hydrazine hydrate 80% (Merck), *p*-nitrophenol (PNP) (Merck), and *p*-aminophenol (PAP) (as a standard materials), ethanol (spectroscopic grade) (Merck) were used.

### Preparation of SiO<sub>2</sub>-Al<sub>2</sub>O<sub>3</sub> Mixed Oxide Support

SiO<sub>2</sub>-Al<sub>2</sub>O<sub>3</sub> mixed oxide support material was prepared by a sol-gel technique. A 2SiO<sub>2</sub>:3Al<sub>2</sub>O<sub>3</sub> molar ratio batch of the support was prepared by slow hydrolysis. After gelling and drying the sample was calcined at 500 °C for 2 h in order to remove the residual nitrates and volatiles. The resulted solid is designated as SA-500. The sample was then milled using agate mortars and heated at 1000 and 1500 °C for 4 h. The resultant solids are named as SA-1000, and SA-1500, respectively. The surface areas of the prepared supports were 50, 20, 10 m<sup>2</sup>g<sup>-1</sup> for the supports SA-500, SA-1000, and SA-1500, respectively.

### Preparation of Nano-Sized Nickel Catalyst

Nickel was loaded on the supports, previously calcined at 500, 1000 and 1500 °C, by means of impregnation. The amount of Ni was fixed at 5 wt%. Reduction was done using hydrazine hydrate in an alkaline medium at 80–100 °C in order to obtain the metallic form of nickel.

### Hydrogenation Process

The catalytic hydrogenation reaction was done by dissolving 0.1 mol of *p*-nitrophenol in an appropriate amount of ethanol (25 mL), followed by addition of 10 mL hydrazine hydrate as hydrogen source, then heating at 80 °C. The catalyst was added to the heated solution and the time to reach 100% conversion was taken as an expression of the catalytic activity. The catalyst:reactant (PNP) was fixed at a 1:5 molar ratio. The filtrate was then taken and evaporated under reduced pressure. The residue was recrystallized from

hot water to give the pure product of PAP in almost 100% yield.

### X-Ray Diffraction (XRD)

X-ray diffractograms of the various solids were collected using Bruker D8 advance instrument with a CuK $\alpha$ 1 target with secondary monochromator 40 kV, 40 mA.

### ESR Spectroscopy

ESR spectra of the different solids were measured using a Bruker Elexsys 500 operating in the X-band frequency. The following parameters are generalized to all samples unless otherwise mentioned in the text. Microwave frequency: 9.73 GHz, receiver gain: 20, sweep width: 6000 center at 3480, microwave power: 0.00202637.

### SEM and EDX Analysis

Scanning electron microscopy (SEM) images of different samples and EDX analyses was performed using a "JXA-840 A electron probe micro analyzer, Japan" instrument.

### Surface Area Measurements

The surface areas were measured using a Quantachrome High Speed Gas Adsorption Nova 2000 instrument at 77 K.

## References

- [1] K. Okada, *J. Eur. Ceram. Soc.* **2008**, *28*, 377.
- [2] M. A. Ermakova, D. Y. Ermakov, *Appl. Catal. A*: **2000**, *201*, 61.
- [3] J. L. Sebedio, G. Finke, R. G. Ackman, *Chem. Phys. Lipids* **1984**, *34*, 215.
- [4] S. M. Echeverria, V. M. Andres, *Appl. Catal.* **1990**, *66*, 73.
- [5] M. T. Rodrigo, L. Daza, S. Mendioroz, *Appl. Catal. A: Gen.* **1992**, *88*, 101.
- [6] M. W. Balakos, E. E. Hernandez, *Catal. Today*, **1997**, *35*, 415.
- [7] I. H. Abd El Maksoud, *Preparation and Regeneration of Catalysts used in Hydrogenation of Edible Oil*, Ph.D. Thesis, Ain Shams University, **2005**.
- [8] M. M. Selim, I. H. Abd El-Maksoud, *Microporous Mesoporous Mater.* **2005**, *85*, 273.
- [9] C. V. Rode, M. J. Vaidya, R. Jaganathan, R. V. Chaudhari, *Chem. Eng. Sci.* **2001**, *56*, 1299.
- [10] C. V. Rode, M. J. Vaidya, R. V. Chaudhari, *Org. Process Res. Dev.* **1999**, *3*, 465.
- [11] T. Komatsu, T. Hirose, *Appl. Catal. A: Gen.*, **2004**, *276*, 95.
- [12] S. S. Sathe, *Process for preparing p-aminophenol in the presence of dimethyldodecylamine sulfate*, U.S. Patent 4,176,138, **1979**.
- [13] L. T. Lee, M. H. Chen, C. N. Yao, *Process for manufacturing p-aminophenol*, U.S. Patent 4,885,389, **1989**.
- [14] K. S. Yun, B. W. Cho, *Process for preparing paraaminophenol*, U.S. Patent 5,066,369, **1991**.
- [15] M. J. Vaidya, S. M. Kulkarni, R. V. Chaudhari, *Org. Process Res. Dev.* **2003**, *7*, 202.
- [16] K. Venkatraman, *The Chemistry of Synthetic Dyes*, Academic Press, New York, Vol. I, **1952**.
- [17] H. O. House, *Modern Synthetic Reactions*, 2<sup>nd</sup> edn., Benjamin, New York, **1977**.
- [18] P. N. Rylander, *Hydrogenation Methods*, Academic Press, New York, **1985**.
- [19] F. D. Popp, H. P. Schultz, *Chem. Rev.* **1962**, *62*, 19.
- [20] R. E. Harmon, S. K. Gupta, D. J. Brown, *Chem. Rev.* **1972**, *72*, 21.
- [21] R. Z. Chen, Y. Du, C. L. Chen, W. H. Xing, N. P. Xu, C. X. Chen, Z. L. Zhang, *J. Chem. Ind. Eng. (China)* **2003**, *54*, 704.
- [22] Y. Du, H. L. Chen, R. Z. Chen, N. P. Xu, *Appl. Catal. A: Gen.* **2004**, *277*, 259.
- [23] P. A. Rautanen, J. R. Aittamaa, A. O. I. Krause, *Chem. Eng. Sci.* **2001**, *56*, 1247.
- [24] D. J. Suh, T. J. Park, S. H. Lee, K. L. Kim, *J. Non-Cryst. Solids* **2001**, *285*, 309.
- [25] W. H. Wu, J. Xu, *Catal. Commun.* **2004**, *5*, 591.
- [26] W. H. Wu, J. Xu, R. Ohnishi, *Appl. Catal. B: Environ.* **2005**, *60*, 129.
- [27] M. P. Kapoor, Y. Matsumura, *J. Mol. Catal. A: Chem.* **2002**, *178*, 169.
- [28] S. Toppinen, T. K. Rantakyh, T. Salmi, J. Aittamaa, *Catal. Today* **1997**, *38*, 23.
- [29] C. E. Quincoces, M. G. Gonzfilez, *Chin. J. Chem. Eng.* **2001**, *9*, 190.
- [30] C. Rizhi, D. Yan, X. Weihong, X. Nanping, *Chin. J. Chem. Eng.* **2006**, *14*, 665.
- [31] S. Gowda, D. C. Gowda, *Tetrahedron* **2002**, *58*, 2211.
- [32] C. V. Rode, M. J. Vaidya, R. V. Chaudhari, *Org. Process Res. Dev.* **1999**, *3*, 465.
- [33] I. H. Abd El Maksod, T. S. Saleh, *Green Chem. Lett. Rev.* **2009**, accepted for publication.
- [34] A. Kawabata, *J. Phys. Soc. Jpn.* **1970**, *29*, 902.
- [35] V. K. Sharma, A. Baiker, *J. Chem. Phys.* **1981**, *75*, 5596.
- [36] G. Suran, A. Stankoff, F. Hofmann, *Phys. Rev. B* **1973**, *8*, 1109.